

A SEQUENTIAL CONTROL FOR WIND TURBINE GENERATING SYSTEMS TO MITIGATE TORQUE PULSATIONS DURING UNBALANCED CONDITIONS

¹Mihir Mehta, ²Alpesh Parmar, ³Bhinal Mehta

¹Assistant Professor, ²Student, ³Associate Professor

¹M & V patel Department of Electrical Engineering,

¹C. S. Patel Institute of Technology, Charotar University of Science & Technology, Changa, Anand, Gujarat-388421, India

Abstract: Several technical challenges are observed during grid integrations with the renewable power system comprising of models which precisely reckon of short circuit contributions and system protection studies. Compared to traditional generators, Wind Turbine Generators (WTGs) integrated through converter produce different current and power waveforms which may contain harmonics during normal as well as abnormal conditions. This paper proposes a sequential control topology that eliminate the second harmonic components and accounts for impacts on electromagnetic torque, active and reactive power with Doubly Fed Induction Generator (DFIG) under different fault conditions.

Index Terms - Doubly Fed Induction Generator, Second Order Harmonics, Wind Turbine Generators, Unbalanced Faults.

I. INTRODUCTION

Modern Wind Parks (WPs) install variable speed wind turbines (WTs) in order to absorb maximum wind energy and fulfill the grid code requirement and also reducing the drive train stress. Integrating large scale WP with the grid has several issues and has sever impacts on power system transient behavior. Failing to which not only leads to un-optimized design and operations of WPs but also problems of grid operation and stability. Majority of research work is carried on time domain behavior of short circuit characteristics of WTs [1]-[5] as well as on dynamic phasor modeling [6]-[8] of generators coupled electronically. This paper demonstrates the behavior of electromechanical torque, active power, and reactive power as well as positive and negative sequence current by implementing the proposed sequential control scheme which eliminates the second harmonic component in comparison to conventional control scheme. The paper comprises of following sections: Modeling of DFIG WTGs, Conventional control scheme, proposed control scheme, Test system and test cases, Results and discussions, Conclusion.

II. MODELING OF DFIG WIND TURBINE GENERATORS

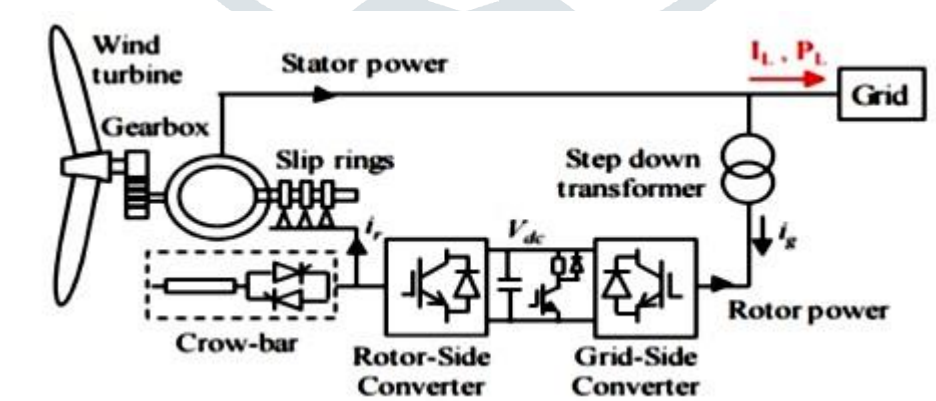


Figure 1 DFIG WT configuration

As shown in Fig. 1 in DFIG WTGs, grid is directly connected to the stator of the generator while connections made to the rotor are through AC-AC converter system. Converter comprises of three-phase PWM converters, Grid Side Converters (GSC) coupled to Rotor Side Converter (RSC) through a DC bus. Vector control technique is used for controlling the GSC and RSC. This further allows the control of active and reactive power through proposed control. Based on AC flux or voltage, the projection of d- and q-current components are made on rotating reference frame. Real power and reactive power are represented by q-component and d-component of flux based rotating reference frame. As the flux-based reference frame lags by 90° to voltage-based frame, representation of d and q component interchanges.

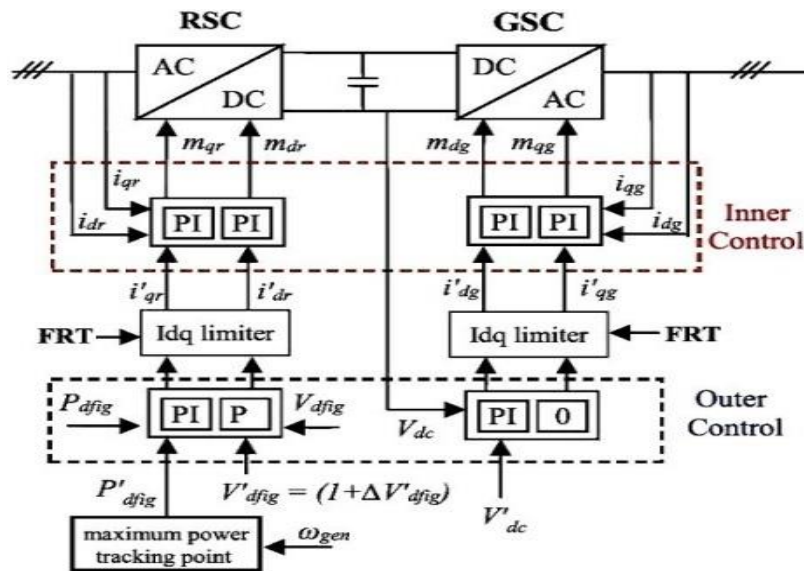


Figure 2 DFIG WT control scheme

The Fig. 2 shows the control model of DFIG WTs. The d-axis and q-axis current of RSC and GSC are given by i_{dr} , i_{qr} , i_{dg} and i_{qg} respectively. The DC bus voltage, active power of DFIG and its positive sequence terminal voltage are given by V_{dc} , P_{dfig} and V_{dfig} respectively. In the proposed control system RSC and GSC operated in stator flux reference frame (SFR) and stator voltage reference frame (SVR) respectively. RSC parameters like i_{dr} holds the responsibility of controlling P_{dfig} while i_{qr} is responsible for controlling V_{dfig} whereas GSC parameters like i_{dg} holds responsibility of controlling the DC bus voltage and i_{qg} supports with reactive power to the grid during faults. There are two control loops i.e the outer control loop and the inner control loop. The outer control loop calculated the reference d-axis and q-axis currents (i_{dr} , i_{qr} , i_{dg} and i_{qg}) while the inner loop controls the reference AC voltage of the converters which would be used to generate modulated switching pattern. The references for active power of DFIG (P'_{dfig}) and positive sequence voltage of DFIG (V'_{dfig}) is provided by MPPT algorithm and Wind Park Control (WPC). The reactive power control of the wind parks is based on the concept of secondary voltage control. The outer control loop of WTs follows the voltage references sent by Wind Park Control (WPC) as shown in Fig. 3.

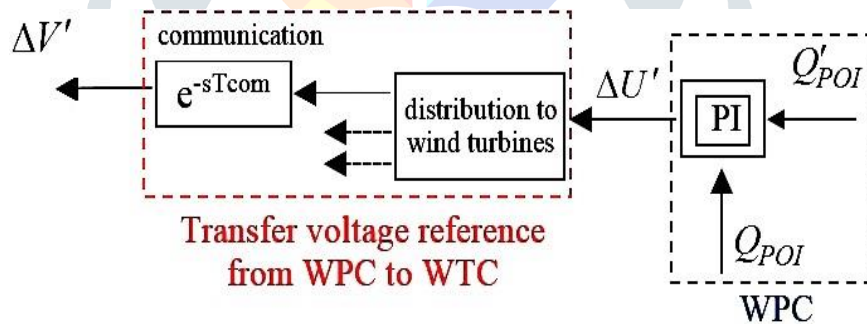


Figure 3 Reactive power control at POI

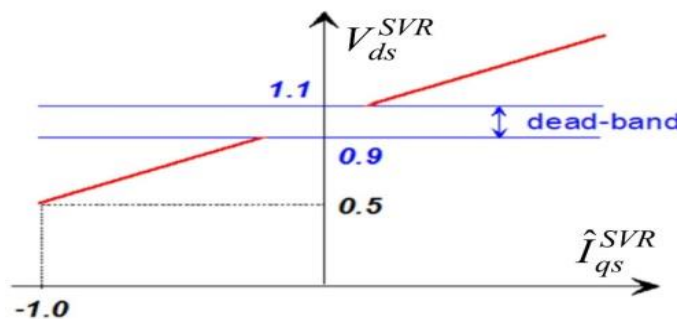


Figure 4 Reactive output current of WT during voltage sags

The proportional integral (PI) regulator helps in achieving the desired reactive power flow at the Point Of Interconnection (POI). If WPC is operating under V-control function mode, then the reactive power reference (Q'_{POI}) is calculated using

$$Q'_{POI} = K_{Vpoi} (V'_{POI} - V_{POI}) \tag{2.1}$$

where V_{POI} and K_{Vpoi} are the positive sequence voltage at POI and the voltage regulated gain at WPC respectively. If WPC is operating under power factor (PF) control function, the reactive power reference (Q'_{POI}) is computed using active power at POI

(P_{POI}) as well as desired power factor at POI (PF'_{POI}). The PI regulator output ($\Delta V'_{dfig}$) is kept constant by blocking the input ($Q'_{POI} - Q_{POI}$) to avoid overvoltage following the removal. The WT's are also equipped with Fault-Ride-Through (FRT) function to fulfill grid code requirements as shown in the Fig. 4 and is activated (V_{FRT-ON}) when voltage deviation exceeds its pre-defined value from 1 pu and deactivated ($V_{FRT-OFF}$) when the voltage deviation reduces below pre-defined value. Reactive current is injected by DFIG in proportion to voltage deviation from 1pu when FRT function is in active mode.

III. CONVENTIONAL CONTROL SCHEME OF DFIG

The q-axis reference current is calculated by outer voltage control loop, as follows

$$i'_{qg} = K_v (V'_{dfig} - V_{dfig}) - (I_{dr}^{lim} - i_{dr-m}) \tag{3.1}$$

Here K_v is the voltage regulator gain, i_{dr-m} is the reactive current absorbed by DFIG.

$$i_{dr-m} = V_{dfig} / (\omega_s L_m) \tag{3.2}$$

where L_m denotes magnetizing inductance of induction generator and V_{dfig} is the positive sequence voltage at DFIG WT terminals. The PI regulator calculates d-axis and q-axis reference voltage for the converters by using feed forward compensating terms $\omega L_{choke} i_{qg} + v_{d-choke}$ and $(-\omega L_{choke} i_{dg} + v_{q-choke})$ as follows

$$v'_{dg} = - \left(k_p + \frac{k_i}{s} \right) (i'_{dg} - i_{dg}) + \omega L_{choke} i_{qg} + v_{d-choke} \tag{3.3}$$

$$v'_{qg} = - \left(k_p + \frac{k_i}{s} \right) (i'_{qg} - i_{qg}) - \omega L_{choke} i_{dg} + v_{q-choke} \tag{3.4}$$

Priority is given to active currents by the controller during normal operations

$$i'_{dg} < I_{dg}^{lim} \tag{3.5}$$

$$i'_{qg} < I_{qg}^{lim} = \sqrt{(I_g^{lim})^2 - (i'_{dg})^2} \tag{3.6}$$

Where, I_{dg}^{lim} and I_{qg}^{lim} represents the d-axis and q-axis currents whereas I_g^{lim} represents the total GSC currents. The FRT function is activated when

$$|1 - V_{dfig}| > V_{FRT-ON} \tag{3.7}$$

and deactivated when

$$|1 - V_{dfig}| < V_{FRT-OFF} \tag{3.8}$$

By reversing the d-axis and q-axis current limit, GSC controller provides priority to the reactive current when FRT function is active

$$i'_{qg} < I_{qg}^{lim} \tag{3.9}$$

$$i'_{dg} < I_{dg}^{lim} = \sqrt{(I_g^{lim})^2 - (i'_{qg})^2} \tag{3.10}$$

IV. PROPOSED CONTROL SCHEME OF DFIG

During unbalanced loading conditions or faults, the terminal voltage of DFIG WT contains negative sequence components which lead to second harmonic oscillations in GSC power output. The instantaneous active and reactive power in unbalanced grid conditions can be also written as [9].

$$p = P_0 + P_{C2} \cos(2\omega t) + P_{S2} \cos(2\omega t) \tag{4.1}$$

$$q = Q_0 + Q_{C2} \cos(2\omega t) + Q_{S2} \cos(2\omega t) \tag{4.2}$$

Where P_0 represents the average value of instantaneous active power and Q_0 is the average values of the instantaneous reactive powers. P_{C2} , P_{S2} , Q_{C2} , Q_{S2} represent the magnitude of the second harmonic oscillating terms in the Eq.(4.1) and Eq.(4.2). The amplitude of these power magnitudes can be calculated as follows:

$$P_0 = \frac{3}{2} (v_d^+ i_d^+ + v_q^+ i_q^+ + v_d^- i_d^- + v_q^- i_q^-) \tag{4.3}$$

$$P_{C2} = \frac{3}{2} (v_d^- i_d^+ + v_q^- i_q^+ + v_d^+ i_d^- + v_q^+ i_q^-) \tag{4.4}$$

$$P_{S2} = \frac{3}{2} (v_q^- i_q^+ - v_d^- i_d^+ - v_q^+ i_q^- + v_d^+ i_d^-) \tag{4.5}$$

$$Q_0 = \frac{3}{2} (v_q^+ i_d^+ - v_d^+ i_q^+ + v_q^- i_d^- - v_d^- i_q^-) \tag{4.6}$$

$$Q_{C2} = \frac{3}{2} (v_q^- i_d^+ - v_d^- i_q^+ + v_q^+ i_d^- - v_d^+ i_q^-) \tag{4.7}$$

$$Q_{S2} = \frac{3}{2} (-v_d^- i_d^+ - v_d^- i_q^+ - v_q^+ i_d^- + v_q^+ i_q^-) \tag{4.8}$$

Where i_d^+, i_q^+ and v_d^+, v_q^+ are calculated by Park transform [10] and represent the dq components of the positive-sequence current and voltage vectors expressed in synchronous reference frame, whereas i_d^-, i_q^- and v_d^-, v_q^- are the components of the negative-sequence current and voltage respectively on a synchronous reference frame rotating at same speed as in positive sequence component but in opposite direction. For a given grid voltage conditions, P_{S2} , P_{C2} , Q_{S2} and Q_{C2} can be controlled with proposed control method. Active power terms P_{C2} , P_{S2} cause oscillations in DC bus voltage V_{dc} . In order to nullify P_{C2} & P_{S2} , GSC current references ($i_{dg}'^+, i_{qg}'^+, i_{dg}'^-, i_{qg}'^-$) are recalculated.

The I_{dq} limiter and outer control calculate $i'_{dg}, i'_{qg}, i_{dg}^{lim}, i_{qg}^{lim}$ and further calculate the GSC current references $i_{dg}^{+'}, i_{qg}^{+'}, i_{dg}^{-'}, i_{qg}^{-'}$ for the proposed current controller. During the fault, positive sequence reactive current injection is defined by the grid code and hence the GSC current references are calculated [6] as below:

$$\begin{bmatrix} i_{qg}^{+'} \\ i_{dg}^{+'} \\ i_{qg}^{-'} \\ i_{dg}^{-'} \end{bmatrix} = \begin{bmatrix} 1 & 0 & 0 & 0 \\ v_{qg}^{+} & v_{dg}^{+} & v_{qg}^{-} & v_{dg}^{-} \\ v_{qg}^{-} & v_{dg}^{-} & v_{qg}^{+} & v_{dg}^{+} \\ -v_{dg}^{-} & v_{qg}^{-} & v_{dg}^{+} & -v_{qg}^{+} \end{bmatrix}^{-1} \begin{bmatrix} i'_{qg} \\ P_0 \\ P_{C2} \\ P_{S2} \end{bmatrix} \quad (4.9)$$

Where P_0 is given by

$$P_0 = i'_{qg} V'_{wt} \quad (4.10)$$

Keeping due care of the converter limit I_{dg}^{lim} and I_{qg}^{lim} , the reference values of Eq.(4.9) are recalculated. The priority is providing I_{dg}^{+} as specified by grid code specially during fault conditions. The remaining reserve of GSC are used in elimination of P_{C2} and P_{S2} . Thus, the performance deteriorates with the decrease in electrical distance between the fault location and the WP.

V. TEST SYSTEM AND TEST CASES

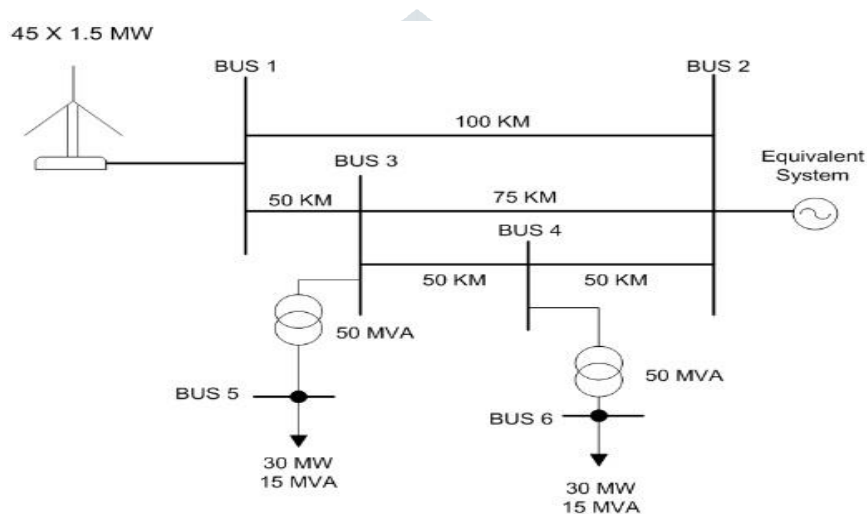


Figure 5. 120 KV Test System

Table 1 Simulation Cases of WP with DFIG WT

| Fault Location | Case | Type of Fault | Control Scheme |
|----------------|--------|---------------|----------------------|
| Bus 4 | Case A | LG Fault | Conventional Control |
| | | | Proposed Control |
| | Case B | LLG Fault | Conventional Control |
| | | | Proposed Control |
| | Case C | LLL Fault | Conventional Control |
| | | | Proposed Control |

Figure 5 shows single line diagram of the 120KV, 60 Hz test system of WP having installed capacity of 67.5 MW comprising of 45 WTs each having capacity of 1.5 MW DFIG operating at full load under unity power factor ($Q_{POI} = 0$). The loads connected from bus to ground on each phase and are represented by equivalent impedance. Distributed constant parameters models are used to represent transmission lines. Table 1 represents the simulation cases for different types of faults at Bus 4. The different fault cases are also simulated at different location but due to the space constraint it is not shown. The similar results are obtained for fault at Bus 6.

VI. RESULTS AND DISCUSSION

Figure 6, Figure 7 and Figure 8 shows the comparative responses in per unit for the electromagnetic torque, active power, reactive power, positive and negative sequence currents for conventional and proposed schemes for all three types of faults i.e LG, LLG and LLLG respectively. The fault is initiated at 2 seconds and it is cleared after 250ms. It is clearly depicted from the Fig. 6 and Fig. 7 that the proposed sequential control scheme reduces the second harmonic pulsation in the electromechanical torque which is present in asymmetrical fault. The negative sequence current compensates the second harmonic components and tries to make it zero. It can also be concluded from Fig. 8 that the second harmonic component is absent because of symmetrical fault (LLL) and thus proposed and conventional scheme have the similar responses. The active and the reactive power outputs are almost similar for conventional and proposed control scheme except the amplitude of the variation is slightly less in the proposed scheme compared to the conventional scheme. A higher value of negative sequence fault current is obtained using the proposed scheme compared to conventional scheme.

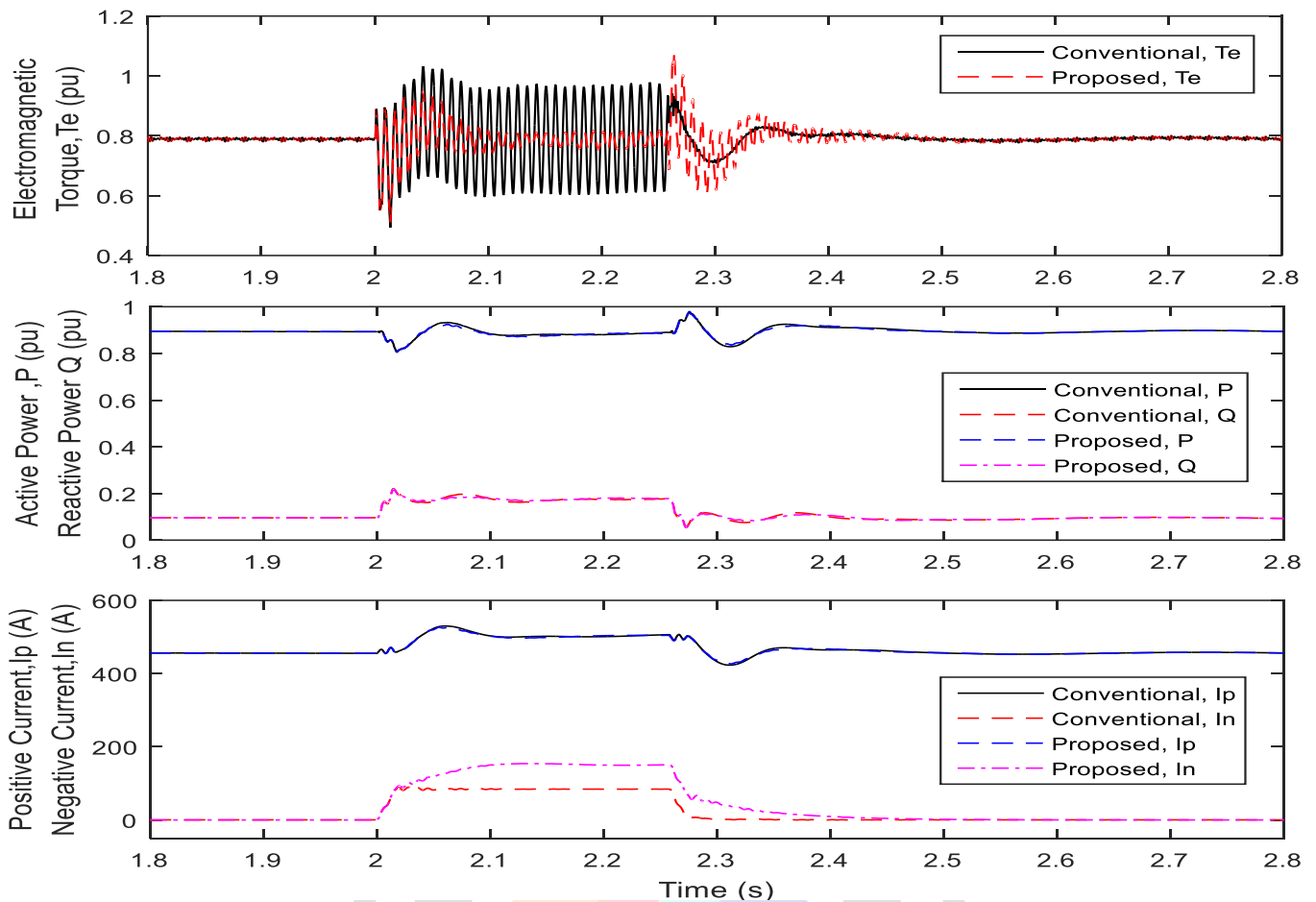


Figure 6 Results for Case A

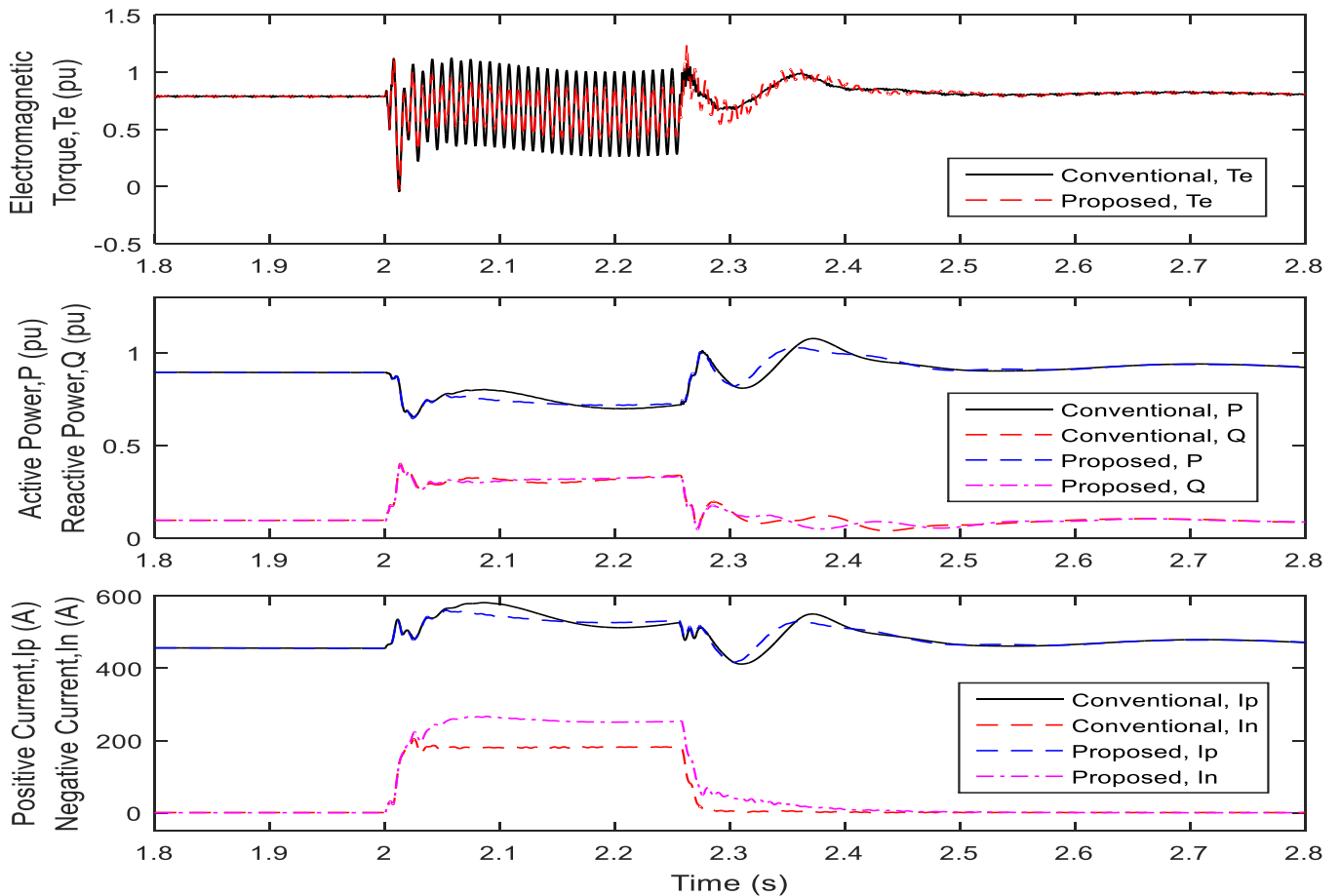


Figure 7 Results for Case B

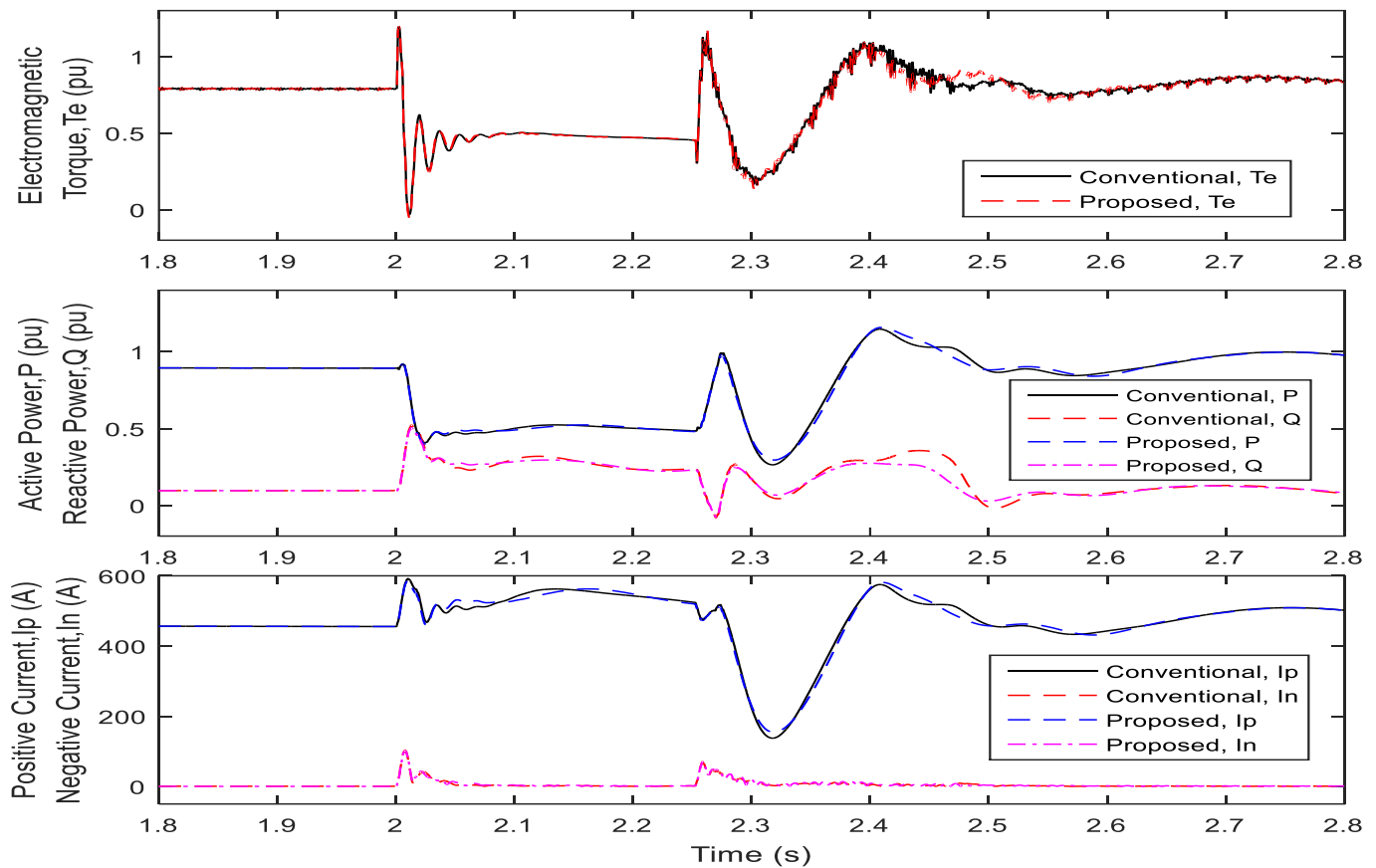


Figure 8 Results for Case C

VII. CONCLUSION

This paper presents a proposed control scheme which can be adopted for short circuit analysis of any type of wind turbine generating system having electronically coupled generator. WT are expected to be equipped with a DC resistance chopper which limits the DC voltage, avoids crowbar ignition and deliver continuous control of DFIG during faults that occur outside WP. Impact of WT control is responsible to provide solution in both normal operating mode as well as fault-ride-through operating mode. The proposed control scheme helps in stabilizing the electromechanical torque, increase the negative sequence current and lower the peak variations in active and reactive power. Results are validated by simulating various fault condition at different locations and comparing the results of proposed control scheme to conventional control scheme. Additionally, the proposed control scheme is also flexible to FRT capabilities.

VIII. REFERENCES

- [1] E. Muljadi and V. Gevorgian, "Short-circuit modelling of a wind power plant," Proc. IEEE Power Eng. Soc. Gen. Meeting, Detroit, MI, USA, Jul. 2011, pp. 1–9.
- [2] J. Martinez, P. C. Kjar, P. Rodriguez, and R. Teodorescu, "Short circuit signatures from different wind turbine generator types," Proc. IEEE Power Syst. Conf. Expo., Phoenix, AZ, USA, Mar. 2011, pp. 1–7.
- [3] R. A. Walling, E. Gursay, and B. English, "Current contribution from type 3 and type 4 wind turbine generators during faults," Proc. IEEE Power Eng. Soc. Gen. Meeting, Detroit, MI, USA, Jul. 2011, pp. 1–6.
- [4] E. Farantatos, U. Karaagac, H. Saad, and J. Mahseredjian, "Short-circuit current contribution of converter interfaced wind turbines and the impact on system protection," in Proc. BulkPower Syst. Dyn. Control—IX Security Control Emerging Power Grid, Rethymno, Crete, Greece, Aug. 2013, pp. 1–9.
- [5] M. Chen, L. Yu, N. S. Wade, X. Liu, Q. Liu, and F. Yang, "Investigation on the faulty state of DFIG in a microgrid," in IEEE Trans. Power Electron., vol. 26, no. 7, pp. 1913–1919, Jul. 2011.
- [6] T. Demiray, F. Milano, and G. Andersson, "Dynamic phasor modeling of the doubly-fed induction generator under unbalanced conditions," in Proc. IEEE Power Tech, Lausanne, Switzerland, 2007, pp. 1049–1054.
- [7] S. Chandrasekar and R. Gokaraju, "Dynamic phasor modeling of type 3 DFIG wind generators (including SSCI phenomenon) for short-circuit calculations," IEEE Trans. Power Del., vol. 30, no. 2, pp. 887–897, Apr. 2015.
- [8] A. El-Naggar and I. Erlich, "Fault current contribution analysis of doubly fed induction generator-based wind turbines," IEEE Trans. Energy Convers., vol. 30, no. 3, pp. 874–882, Sep. 2015.
- [9] R. Teodorescu, M. Liserre, P. Rodriguez, Grid Converters for Photovoltaic and Wind Power Systems, 2011, IEEE/Wiley.
- [10] Park, R.H., 'Tow Reaction Theory of Synchronous Machines. Generalized Method of Analysis – Part I'. In Proceedings of Winter Convention of AIEE, 1929, pp. 716–730.